COMPDYN 2013
4th ECCOMAS Thematic Conference on
Computational Methods in Structural Dynamics and Earthquake Engineering
M. Papadrakakis, V. Papadopoulos, V. Plevris (eds.)
Kos Island, Greece, 12–14 June 2013

A NEW PERFORMANCE-BASED DESIGN METHODOLOGY FOR CONTROLLED ROCKING STEEL FRAMES

Lydell Wiebe[1], **Constantin Christopoulos**[1]

[1] Department of Civil Engineering, University of Toronto
35 St. George Street, Toronto, ON, Canada, M5S 1A4
e-mail: lydell.wiebe@mail.utoronto.ca
e-mail: c.christopoulos@utoronto.ca

Keywords: Controlled rocking steel frames, self-centering systems, higher mode effects, multiple force-limiting mechanisms, performance-based design, capacity design.

Abstract. *The damage caused by recent earthquakes has highlighted the limitations of current seismic force resisting systems and design methodologies, which limit seismic forces by accepting structural damage. Controlled rocking steel frames have been proposed as an alternative system that can limit seismic forces while minimizing structural damage. This paper proposes a new performance-based design methodology for controlled rocking steel frames. In the first step of this methodology, post-tensioning and energy dissipation are designed to achieve target peak displacements at multiple seismic hazard levels. In the second step, the peak force demands on the frame members are estimated using a procedure that is based on the modal properties of cantilever beams with uniformly distributed mass and elasticity. These demands can either be satisfied through elastic design or reduced by using multiple force-limiting mechanisms.*

The proposed design methodology is demonstrated by application to a twelve-storey structure in California. The results of nonlinear time history analyses show that the methodology leads to a design that satisfies the displacement limits, and that it provides good estimates of the peak force demands on the frame members. The methodology also captures the reduction in forces that is achieved by using multiple mechanisms to control the higher mode effects.

1 INTRODUCTION

Events like the 2011 Canterbury earthquake sequence have demonstrated how costly it is to recover from the damage that major earthquakes cause to code-compliant conventional structural systems. Controlled rocking systems (CRS) show great promise for avoiding expensive repairs and lost building use after major earthquakes. These systems exhibit the characteristic flag-shaped hysteresis that is shown in Figure 1, which is defined by an initial stiffness k_0, linear limit f_y, nonlinear stiffness ratio α, and energy dissipation parameter β. Systems with this self-centering hysteresis can be designed to achieve similar peak displacements as conventional systems, while also avoiding residual displacements [1].

In a controlled rocking steel frame, the columns of a frame are allowed to uplift from the foundation, while post-tensioning and energy dissipation devices are used to control the response. Rocking steel frames were first tested in the 1970s [2-4], and recent tests of systems with energy dissipation and post-tensioning have further validated the system [e.g. 5-11]. However, numerical analyses of controlled rocking steel frames have demonstrated that the peak forces are not limited by rocking in the way that would be expected for capacity design [12-14]. Instead, the forces continue to increase as the system rocks because of higher mode effects. This behaviour has recently been demonstrated by large-scale shake table testing [11].

To mitigate the effects of the higher modes, Wiebe et al. [15] proposed using multiple mechanisms to limit the peak seismic forces. Two mechanisms were proposed: designing for rocking to occur at multiple locations over the height of the structure, and designing nonlinear braces at one or more levels to limit the storey shears. Shake table testing demonstrated that both proposals reduce the peak forces with only minor increases in peak displacements [11]. Furthermore, these mechanisms make numerical models more reliable because they reduce the sensitivity to the assumed inherent damping [16].

The purpose of this paper is to give an overview of a new methodology that enables designers to make use of these recent advances in controlled rocking steel frames. Numerical results that validate the methodology will also be presented.

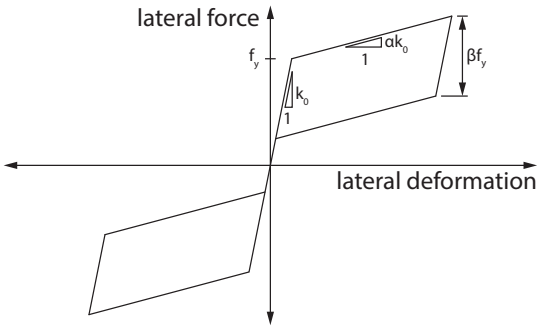

Figure 1: Flag-shaped hysteresis: definition of terms.

2 DESIGN METHODOLOGY

2.1 Overview

Other researchers have proposed designing controlled rocking steel frames with force reduction factors that are similar to the maximum factors in current codes [13-14, 17]. This paper proposes a performance-based design methodology, which is based on two discrete performance levels that are defined following the seismic rehabilitation guidelines of ASCE 41-06 [18]. The first considered performance level is Immediate Occupancy (IO), in which a

building is safe to occupy, although some non-structural repairs may be necessary. The second considered performance level is Collapse Prevention (CP), in which any level of structural damage is accepted except for collapse. In the proposed methodology, these performance levels are associated with the design basis earthquake (DBE, probability of exceedance of 10% in 50 years) and the maximum considered earthquake (MCE, probability of exceedance of 2% in 50 years) levels, respectively. Based on recent events [19], this is considered to be a better reflection of societal expectations than what is currently codified [20-21]. However, these performance targets could be adjusted without affecting the underlying methodology.

Figure 2 summarizes the steps of the proposed design methodology, together with significant limit states for controlled rocking steel systems. The hierarchy of limit states may vary from one CRS to another, depending on the design. The proposed methodology follows the same steps as the design of conventional seismic force resisting systems. Before beginning design, it is necessary to establish the design parameters, such as the seismic hazard, site class, structural layout, and preliminary locations and dimensions of seismic force resisting systems.

With this information, the first step is to proportion the base rocking joint by selecting the amount and location of post-tensioning and energy dissipation, as well as what gravity loads the CRS will carry. Section 2.2 describes a performance-based method for doing this, but other methods could be used without affecting the other steps of the methodology. Higher mode effects and mitigation are not considered in this step because the displacement response of the CRS is intended to be dominated by the base rocking behaviour.

The second step is to capacity design all other elements for elastic response under the maximum expected loads. Because of higher mode effects, these loads cannot be estimated using the properties of the first mode alone. A method for estimating the higher mode effects, which is based on the theoretical modal properties of cantilevered beams with uniformly distributed mass and elasticity, is proposed in Section 2.3. However, other capacity design methods [e.g. 12-14] could be used without affecting the other steps of the methodology. If higher mode effects have a pronounced influence on the capacity design forces, these effects can be mitigated by using multiple force-limiting mechanisms, as will be discussed in Section 2.4.

The third step of the design is to detail the connections. Because of the variability associated with the peak member forces, a double capacity design approach is proposed, with the connections designed for the maximum likely member strengths. Although no capacity-designed elements of the CRS are intended to yield, this step ensures some reserve of ductility by confining any unintentional yielding to the members, rather than the connections.

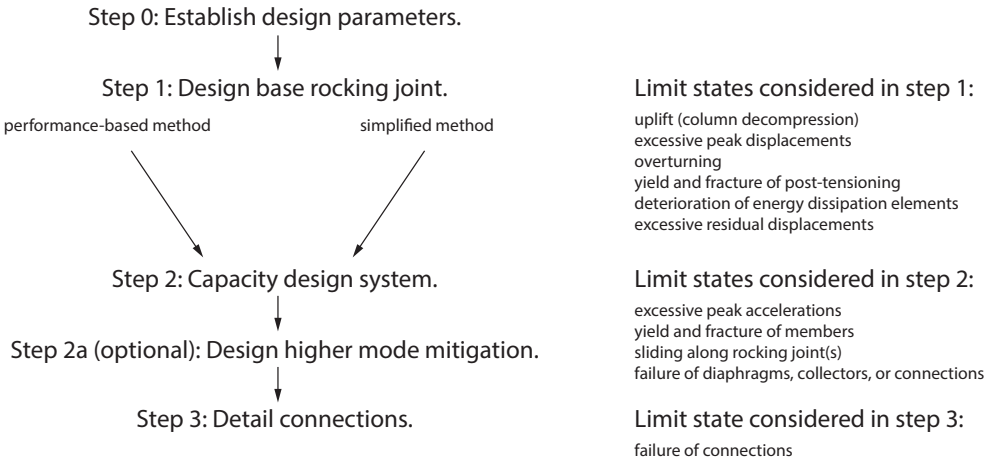

Figure 2: Steps of proposed design methodology.

2.2 Step 1: Design of base rocking joint for displacement-based limit states

To achieve IO at a seismic hazard level, it is necessary to limit the displacements to avoid both non-structural and structural damage. Priestley et al. [22] suggest that peak interstorey drifts of 1.2% could be permitted with proper detailing of non-structural elements. Yielding of the post-tensioning and deterioration of any energy dissipation devices should be prevented at this level. Residual deformations must also be limited to 0.5% [23].

To achieve CP at a seismic hazard level, it is necessary to limit the displacements to avoid failure of the gravity load system and the CRS components. The National Building Code of Canada [21] limits the peak interstorey drifts to 2.5% for most structures under MCE-level ground motions. The maximum expected displacement demands on the post-tensioning and energy dissipation elements must not cause them to fail. P-Δ effects at the maximum expected system displacement must not cause overturning of the CRS.

The above requirements are used to compute maximum allowable interstorey drifts and base rotations at the IO and the CP performance levels. Because the displacements of a CRS are intended to be dominated by the base rocking behavior, the peak interstorey drift is assumed for design to be approximately equal to the peak base rotation, $\theta_{\max}$. At each performance level, this rotation is used to compute the target displacement demand at the effective height of a single-degree-of-freedom (SDOF) model:

$$\Delta_{des} = \theta_{\max} \frac{\sum_{i=1}^{n}\left(m_i h_i^2\right)}{\sum_{i=1}^{n}\left(m_i h_i\right)} \tag{1}$$

where m_i is the tributary seismic mass at storey i, h_i is the height of that storey above the base rocking joint, and n is the number of storeys. The initial period of the system is estimated using approximately 1.4-1.5 times the period given by building codes [20-21]:

$$T_1 = 0.07 h_n^{0.75} \tag{2}$$

where h_n is the height of the structure in meters.

Having determined the target displacement demand and estimated T_1, the next step is to choose hysteretic parameters (f_y, α, and β) that will achieve Δ_{des}. These hysteretic parameters may be chosen using design charts based on the response of SDOF systems with flag-shaped hystereses. Figure 3 shows one such chart, which is based on the median response to the suite of 44 ground motions that was developed for FEMA P695 [24] and scaled to match the maximum MCE-level spectrum in Seismic Design Category D between periods of 0.1 s and 2.0 s. For each ground motion, linear elastic systems with 11 different initial periods were analyzed to determine the peak force demands, and each median demand was divided by a force reduction factor (R) to determine the linear limit (f_y) for an SDOF system with a flag-shaped hysteresis and the same initial period. All of the systems represented in Figure 3 have zero energy dissipation ($\beta = 0$). The nonlinear stiffness ratio, $\alpha = \left(0.1\,\mathrm{s}^{-2}\right)\left(T_1/2\pi\right)^2$, varies with the initial period so that the post-uplift stiffness (αk_0) is independent of the initial period. The post-uplift stiffness can be targeted when designing the base rocking joint, whereas α depends on the initial stiffness, which is known only after the members have been designed. Design charts for other values of α and β are given elsewhere [25].

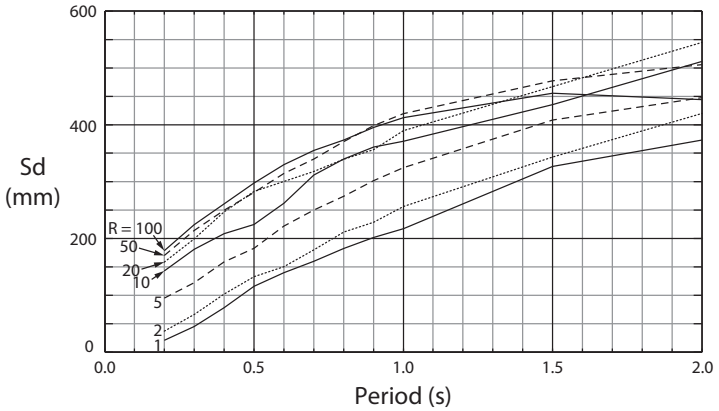

Figure 3: Median peak displacements under MCE-level ground motions: SDOF systems with flag-shaped hysteresis, $\beta = 0$, and $\alpha = \left(0.1\,\mathrm{s}^{-2}\right)\left(T_1/2\pi\right)^2$.

Figure 3 shows an increase in peak displacements with increasing initial period. The peak displacements also tend to increase as the linear limit decreases, but this effect reduces when R is increased beyond about 10. In this range, the peak displacements at some periods reduce when R is increased. This is believed to be because of the statistical error that comes from the limited set of ground motions, and because much of the response of these systems occurs in the nonlinear range, where the instantaneous natural frequency is in the range that is filtered out of the recorded ground motion.

Having selected the force reduction factor, the design base rocking moment is calculated as:

$$M_{b,rock} = \frac{S_a(T_1)}{R} \frac{\left[\sum_{i=1}^{n}(m_i h_i)\right]^2}{\sum_{i=1}^{n}(m_i h_i)} \tag{3}$$

where $S_a(T_1)$ is the design spectral acceleration at the estimated initial period (see equation 2). It is not proposed to allow uplift under any considered level of wind loading. However, it is expected that this requirement could be relaxed if it was shown that many small-amplitude cycles of uplift would not damage the post-tensioning and energy dissipation elements.

Next, the base rocking joint is proportioned to provide the required moment resistance. The contribution from the self-weight on the CRS is calculated first. It is not recommended to have the CRS carry any gravity load other than its self-weight, so as to avoid column force amplification due to impact [26] and to provide better control over the rocking moment in order to minimize the capacity design forces. For preliminary design, the contribution of the frame self-weight can be estimated as 5% of $M_{b,rock}$.

The contribution to the base overturning moment resistance from the energy dissipation, M_{ED}, is designed to achieve the target level of energy dissipation:

$$M_{ED} = M_{b,rock}\left(\frac{\beta}{2}\right) \tag{4}$$

The post-tensioning is selected to provide the remainder of $M_{b,rock}$. The post-uplift stiffness ratio, which was assumed when selecting which design chart to use, must also be verified:

$$\alpha = \frac{\left(A_{PT} E_{PT} / L_{PT}\right) d_{PT}^2 - W_{trib} H_W}{\sum_{i=1}^{n} \left(m_i h_i^2\right)} \left(\frac{T_1}{2\pi}\right)^2 \tag{5}$$

where A_{PT}, E_{PT}, and L_{PT} are the area, modulus of elasticity, and unbonded length of the post-tensioning, respectively, d_{PT} is the horizontal distance from the rocking toe to the location of the post-tensioning, and W_{trib} and H_W are the total tributary seismic weight and the height of its centroid. The peak displacement is not sensitive to the post-uplift stiffness, so it can usually be verified that the value of R that was chosen using an assumed value of α is also adequate when α is determined using equation 5. The energy dissipation and post-tensioning must both be designed to avoid failure at the maximum expected base rotation at the CP performance level (2.5%, unless a different value is used in equation 1). The energy dissipation and post-tensioning are also designed to avoid damage at the maximum expected base rotation at the IO level.

Once the base rocking joint has been designed, the resistance to overturning is checked at the maximum expected base rotation at the CP performance level. To provide an added measure of safety for very large earthquakes, it is recommended that the rocking joint be designed with a slotted connection that causes it to lock up at the maximum expected base rotation. For demands beyond this point, it is expected that the frame would respond similarly to a conventional braced frame, but with an additional rigid body rotation that would reduce the ductility demand. A similar concept for post-tensioned steel frames, in which the connections are capacity designed to confine yielding to the beams, has been experimentally validated [27].

2.3 Step 2: Capacity design of frame for acceleration-based limit states

Because the peak force demands in a CRS are strongly influenced by higher mode effects, these effects must be estimated during design. A method for calculating the design forces has been developed based on the modal properties of cantilever beams with uniformly distributed mass and elasticity, and this method has been calibrated through extensive time history analyses [25]. The method does not require a structural model of the CRS because the equations use only the overstrength base overturning moment resistance ($M_{b,\max}$), the height of each storey above the base (z), the height of the CRS (H), the tributary seismic mass (W_{trib}/g), and the five-percent-damped spectral accelerations at one third and one fifth of the fundamental period ($S_a(T_1/3)$ and $S_a(T_1/5)$). Table 1 lists the equations that are used for the modal contributions to the shear force and overturning moment envelopes ($V_{\max}$ and $M_{\max}$, respectively). To account for uncertainties in the ground motion, the acceleration spectrum is multiplied by a demand factor $\alpha_i \geq 1$. It is proposed that this factor be taken as the ratio of the median-plus-standard-deviation acceleration spectrum to the median spectrum, which is approximately 1.5 for the suite of FEMA P695 records [24] at periods of less than 2 s.

Using the first three modes, the modal contributions are combined by assuming that the peak response is reached in the first mode and sustained, and that the higher modes are superimposed on that first-mode response:

$$V_{\max}(z) = V_{1,\max}(z) + \sqrt{\left(V_{2,\max}(z)\right)^2 + \left(V_{3,\max}(z)\right)^2} \tag{6}$$

$$M_{\max}(z) = M_{1,\max}(z) + \sqrt{\left(M_{2,\max}(z)\right)^2 + \left(M_{3,\max}(z)\right)^2} \tag{7}$$

description	equation
storey shear	
first mode	$V_{1,\max}(z) = \frac{3}{2}\left(\frac{M_{b,\max}}{H}\right)\left[1-\left(\frac{z}{H}\right)^2\right]$
second mode	$V_{2,\max}(z) = 0.1265\left[\alpha_i S_a(T_1/3)\right]\left(\frac{W_{trib}}{g}\right)\left\lvert\cos 4.49\left(\frac{z}{H}\right)+0.217\right\rvert$
third mode	$V_{3,\max}(z) = 0.0297\left[\alpha_i S_a(T_1/5)\right]\left(\frac{W_{trib}}{g}\right)\left\lvert\cos 7.73\left(\frac{z}{H}\right)-0.1283\right\rvert$
overturning moment	
first mode	$M_{1,\max}(z) = M_{b,\max}\left[1-\frac{3}{2}\left(\frac{z}{H}\right)+\frac{1}{2}\left(\frac{z}{H}\right)^2\right]$
second mode	$M_{2,\max}(z) = 0.0282\left[\alpha_i S_a(T_1/3)\right]\left(\frac{W_{trib}}{g}\right)H\left\lvert\sin 4.49\left(\frac{z}{H}\right)+0.976\left(\frac{z}{H}\right)\right\rvert$
third mode	$M_{3,\max}(z) = 0.00384\left[\alpha_i S_a(T_1/5)\right]\left(\frac{W_{trib}}{g}\right)H\left\lvert\sin 7.73\left(\frac{z}{H}\right)-0.991\left(\frac{z}{H}\right)\right\rvert$

Table 1: Summary of modal contributions to design envelopes.

At each storey level, the brace elements are designed to carry the larger of the shear force demands at the top and bottom of that level. Similarly, each pair of vertical elements is designed to carry the larger of the overturning moment demands at the top and bottom of each storey level. In addition, local effects from post-tensioning and energy dissipation anchorages, as well as from rocking, must be considered.

2.4 Step 2a: Design of upper rocking joint to control acceleration-based limit states

If the design envelopes calculated as described in Section 2.3 are dominated by the higher modes, it may be desirable to use additional mechanisms to better control the response. For such mechanisms to be effective, they must activate at a low enough load to limit the response in the higher modes, but they must not activate at too low a load, or else the deformation demand for the system will concentrate at the higher mode mitigation mechanisms. It is proposed that any upper rocking joint be designed to activate at a moment that is at least as large as the moment associated with rocking at the base, assuming a first-mode distribution of lateral loads, and to have an energy dissipation parameter β that is at least as large as at the base joint. Proposals for the design shear force and overturning moment envelopes, as well as for the design of nonlinear braces, are given elsewhere [25].

3 DESIGN AND MODELLING OF 12-STOREY FRAMES

The proposed methodology was used to design a 12-storey structure. The floor plan and storey heights, which are shown in Figures 4a and 4c, have also been used in a recent study to evaluate the FEMA P695 methodology [28]. The acceleration design spectrum is shown in Figure 4b, together with the spectra of the 44 MCE-level ground motions that were scaled to the design spectrum. Figure 4c shows the structural layout of the CRS, which is designed to fit between the gravity columns. Placing the post-tensioning at the edges of the frame and anchoring it at the sixth storey level provided sufficient elongation capacity to reach base rota-

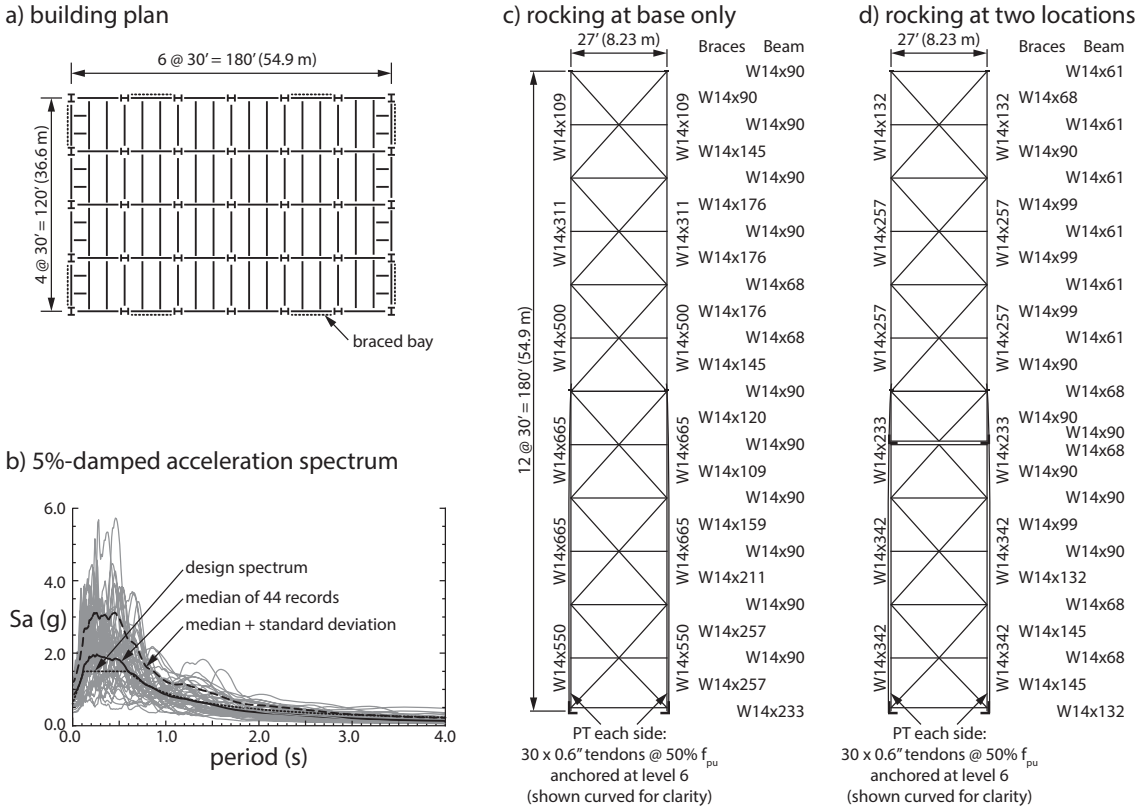

Figure 4: Example design: (a) building plan; (b) 5%-damped acceleration spectrum; (c) summary of design with rocking at base only (US section sizes); (d) summary of design with rocking at two locations (US section sizes).

tions of 1.2% and 2.5% without yield and failure of the post-tensioning, respectively. Therefore, it was not necessary to extend the post-tensioning over the full height of the frame. The target displacement at the CP performance level was calculated using equation 1 as 928 mm, and the fundamental period of the structure was estimated using equation 2 as 1.41 s. At this period, Figure 3 shows that the peak displacement of an SDOF system under the MCE-level suite of ground motions is much less than the maximum allowable displacement, even using a force reduction factor of $R = 100$ and no energy dissipation. Therefore, the CRS is designed with enough post-tensioning to avoid uplift under wind loading, which corresponds to $M_{b,rock} = 32\,800$ kN-m (equivalent to $R = 20.9$) for each frame according to the Directional Procedure of ASCE 7-10 [20].

The capacity design method of Section 2.3 was used to estimate the demands on the frame members, using the median-plus-standard-deviation acceleration spectrum with $\alpha_i = 1$ instead of multiplying the median spectrum by $\alpha_i = 1.5$. As shown in Figure 5, the higher modes dominated the design shear force and overturning moment envelopes. Therefore, an alternative design was considered, in which rocking is allowed not only at the base, but also at the fifth storey. This location was chosen because it is where the estimated second-mode contribution to the overturning moment is largest. No change to the post-tensioning was necessary because of this additional joint, but the member design forces were greatly reduced. The resulting design is shown in Figure 4d; this frame uses 40% less steel than the design with rocking only at the base. An alternative with SCED braces at the first storey was also considered [25] but is not discussed here.

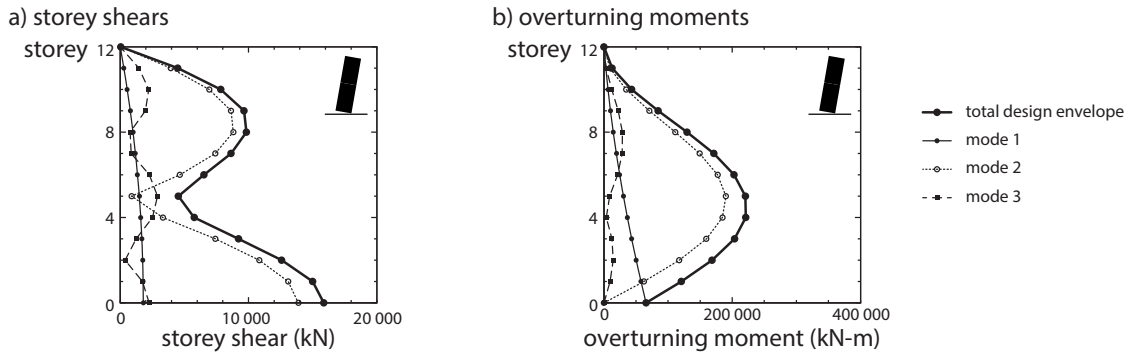

Figure 5: Design envelopes for frame with rocking only at base: (a) storey shears; (b) overturning moments.

Both frames were modelled using OpenSees [29]. The frame members were modelled as linear elastic, but yielding of the post-tensioning elements was modelled with Steel02 elements. The tributary seismic mass was modelled using leaning columns, and the horizontal displacement of the centre node of the frame at each level was slaved to the horizontal displacement of the leaning column at the same level. Five percent tangent stiffness-proportional Rayleigh damping was assigned in the first two modes. The first-mode periods of the frames with rocking only at the base and with two rocking joints were calculated as 1.69 s and 2.24 s, respectively. These periods are larger than the original design estimate of 1.41 s.

4 RESPONSE OF FRAMES TO MCE-LEVEL GROUND MOTIONS

4.1 Peak displacements

To evaluate the ability of the first step of the methodology to target the desired peak displacements at the CP performance level, Figure 6 shows the peak interstorey drifts for both frames during the suite of MCE-level records. The median and median-plus-standard-deviation responses are shown in each figure, both calculated assuming a lognormal distribution. As expected, the median peak interstorey drifts are less than the design limits for both frames, despite the low rocking load that was assigned. Additional analyses confirmed that the displacement response at the IO performance level was also less than the design target [25]. For the frame with an upper rocking joint, one record caused instability in the numerical model after attaining a roof displacement of approximately 10%. This is because the recommended lock-up device, which is intended to prevent collapse under extreme ground motions, was not included in the numerical model.

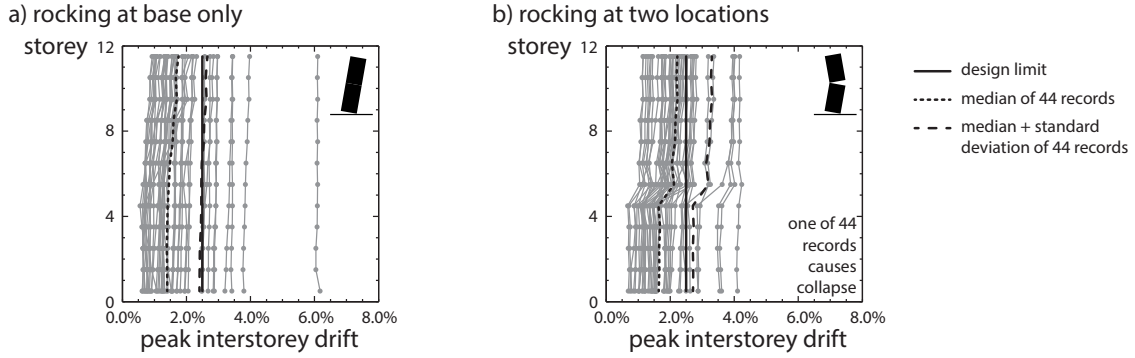

Figure 6: Peak interstorey drifts: (a) rocking at base only; (b) rocking at two locations.

For both frames, the residual displacements were zero after nearly all records. For two MCE-level records, yielding of the post-tensioning reduced the self-centering ability of both frames enough that P-Δ effects caused residual displacements. Nevertheless, this still satisfied the design objectives of IO after a DBE-level record and CP after an MCE-level record.

4.2 Peak forces

To evaluate the ability of the second step of the methodology to capacity design the frame members, Figure 7a shows the peak brace compression demands for the frame with rocking only at the base and Figure 7b shows the peak column compression demands. The design estimates of the peak brace forces are in very good agreement with the median-plus-standard-deviation results from the analyses. The design estimates of the peak column compression demands are good for the upper half of the frame but more conservative than desired for the lower half of the frame. Considering the consequences of member failure and the simplicity of the proposed design method, this extra conservatism is considered acceptable.

Figures 7c-d show the peak brace and column compression demands for the frame with two rocking joints. The median peak forces are substantially reduced by the upper joint. Moreover, the record-to-record variability in the peak response is much less than it was with rocking only at the base because of the increased control provided by the upper joint. The capacity design method produces reasonably good estimates of the peak forces in the braces in the lower half of the frame. As was observed for the frame with rocking only at the base, the design method is more conservative than desired for the columns. However, the method still captures the reduction in force demands for this frame relative to the one with rocking only at the base.

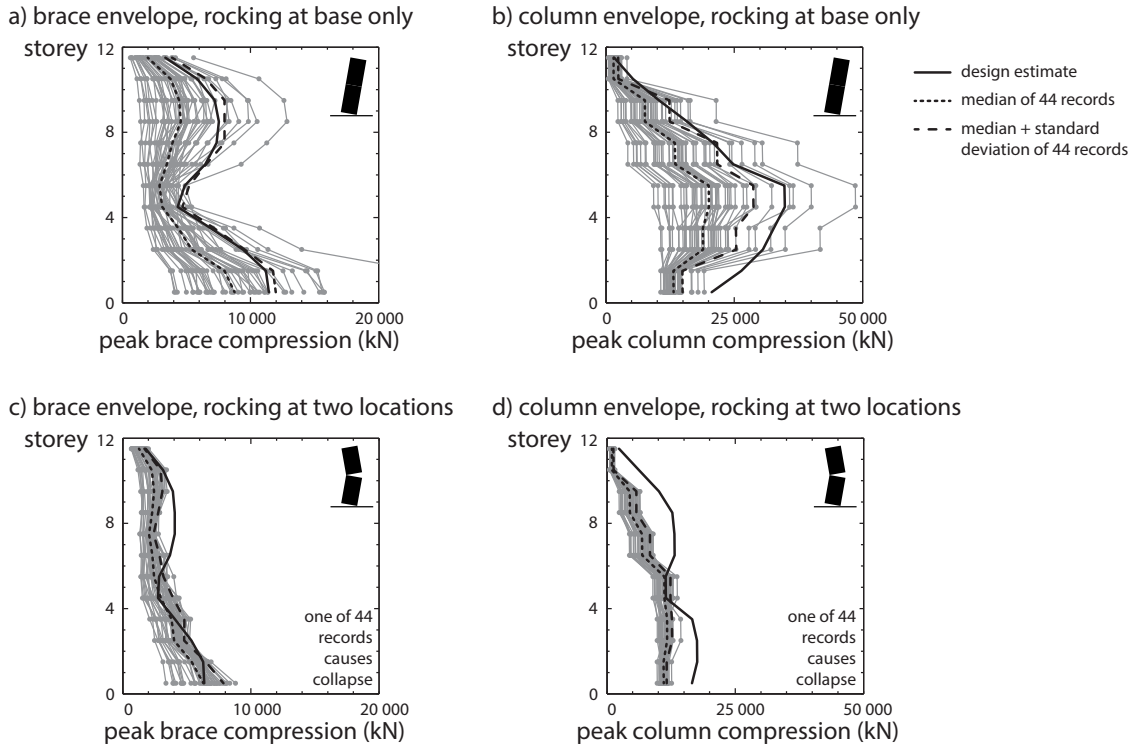

Figure 7: Member compressive force envelopes: (a) braces, rocking at base only; (b) columns, rocking at base only; (c) braces, rocking at two locations; (d) braces, rocking at two locations.

5 CONCLUSION

A new design methodology has been proposed for controlled rocking steel frames. In the first step of the methodology, the base rocking joint is designed to target the desired peak displacements. The proposed method uses an SDOF representation of the system, together with design charts. The method does not require iteration, although an improved response prediction could be obtained by replacing the estimated first-mode period with a period from a structural model. In the second step of the methodology, the frame members are capacity designed for the maximum expected forces, including the effects of the higher modes. Equations were presented that allow these forces to be estimated using only properties that are known during preliminary design.

Two 12-storey frames were designed, one with rocking only at the base and the other with two rocking joints. Nonlinear time history analyses of these frames confirmed that the methodology resulted in designs that achieved the displacement targets. The peak member forces were estimated well or slightly conservatively. The beneficial effect of adding an upper rocking joint was captured by the design method.

This paper has presented a simple and effective way for designers to apply the beneficial effects of controlled rocking. Forthcoming papers will discuss the development and validation of this design methodology more fully. Ongoing research seeks to further refine the methodology, to extend it to other structural systems, and to develop improved details for controlled rocking steel frames.

REFERENCES

[1] C. Christopoulos, A. Filiatrault, B. Folz. Seismic response of self-centring hysteretic SDOF systems. *Earthquake Engineering and Structural Dynamics*, **31**, 1131-1150, 2002.

[2] J.M. Kelly, D.F. Tsztoo. Earthquake simulation testing of a stepping frame with energy-absorbing devices. *Report UCB/EERC-77/17*. Earthquake Engineering Research Center, University of California, Berkeley, 1977.

[3] R.W. Clough, A.A. Huckelbridge. Preliminary experimental study of seismic uplift of a steel frame. *Report UCB/EERC-77/22*, Earthquake Engineering Research Center, University of California, Berkeley, 1977.

[4] A.A. Huckelbridge. Earthquake simulation tests of a nine story steel frame with columns allowed to uplift. Report *UCB/EERC-77/23*, Earthquake Engineering Research Center, University of California, Berkeley, 1977.

[5] M. Midorikawa, T. Azuhata, T. Ishihara, A. Wada. Shaking table tests on seismic response of steel braced frames with column uplift. *Earthquake Engineering and Structural Dynamics*, **35**, 1767-1785, 2006.

[6] R. Tremblay, L.-P. Poirier, N. Bouaanani, M. Leclerc, V. Rene, L. Fronteddu, S. Rivest. Innovative viscously damped rocking braced frames. *Proceedings of the 14th World Conference on Earthquake Engineering*, Beijing, China, October 12-17, 2008.

[7] M. Eatherton, J. Hajjar, G. Deierlein, X. Ma, H. Krawinkler. Hybrid simulation testing of a controlled rocking steel braced frame system. *Proceedings of the 9th US and 10th Canadian Conference on Earthquake Engineering*, Toronto, ON, July 25-29, 2010.

[8] X. Ma, G. Deierlein, M. Eatherton, H. Krawinkler, J. Hajjar, T. Takeuchi, K. Kasai, M. Midorikawa, T. Hikino. Large-scale shaking table test of steel braced frame with controlled rocking and energy dissipating fuses. *Proceedings of the 9th US and 10th Canadian Conference on Earthquake Engineering*, Toronto, ON, July 25-29, 2010.

[9] R. Sause, J.M. Ricles, D.A. Roke, N.B. Chancellor, N.P. Gonner. Seismic performance of a self-centering rocking concentrically-braced frame. *Proceedings of the 9th US and 10th Canadian Conference on Earthquake Engineering*, Toronto, ON, July 25-29, 2010.

[10] M. Pollino, M. Bruneau. Seismic testing of a bridge steel truss pier designed for controlled rocking. *Journal of Structural Engineering*, **136**, 1523-1532, 2010.

[11] L. Wiebe, C. Christopoulos, R. Tremblay, M. Leclerc. Mechanisms to limit higher mode effects in a controlled rocking steel frame. 2: Large-amplitude shake table testing. *Earthquake Engineering and Structural Dynamics*, Early View, DOI 10.1002/eqe.2258, 2012.

[12] D. Roke, R. Sause, J.M. Ricles, N. Gonner. Damage-free seismic-resistant self-centering steel concentrically braced frames. *Proceedings of the 6th International Conference on Behaviour of Steel Structures in Seismic Areas (STESSA 2009)*, Philadelphia, PA, August 16-20, 2009.

[13] M. Eatherton, J. Hajjar. Large-scale cyclic and hybrid simulation testing and development of a controlled-rocking steel building system with replaceable fuses. *NSEL Report NSEL-025*, Department of Civil and Environmental Engineering, University of Illinois at Urbana-Champaign, 2010.

[14] X. Ma. Seismic design and behavior of self-centering braced frame with controlled rocking and energy-dissipating fuses. *PhD Dissertation*. Stanford University, 2010.

[15] L. Wiebe, C. Christopoulos, R. Tremblay, M. Leclerc. Mechanisms to limit higher mode effects in a controlled rocking steel frame. 1: Concept, modelling, and low-amplitude shake table testing. *Earthquake Engineering and Structural Dynamics*, Early View, DOI 10.1002/eqe.2259, 2012.

[16] L. Wiebe, C. Christopoulos, R. Tremblay, M. Leclerc. Modelling inherent damping for rocking systems: results of large-scale shake table testing. *Proceedings of the 15th World Conference on Earthquake Engineering*, Lisbon, Portugal, September 24-28, 2012.

[17] D.A. Roke. Damage-free seismic-resistant self-centering concentrically-braced frames. *PhD Dissertation*. Lehigh University, 2010.

[18] American Society of Civil Engineers. *Seismic rehabilitation of existing buildings*. ASCE Standard ASCE/SEI 41-06. American Society of Civil Engineers, 2007.

[19] Canterbury Earthquakes Royal Commission. *Final Report, Volume 3: low-damage building technologies*. Royal Commission of Inquiry into Building Failure Caused by the Canterbury Earthquakes, 2012.

[20] American Society of Civil Engineers. *Minimum design loads for buildings and other structures*. ASCE Standard ASCE/SEI 7-10. American Society of Civil Engineers, 2010.

[21] National Research Council Canada. *National building code of Canada, 13th ed*. National Research Council of Canada, 2010.

[22] M.J.N. Priestley, G.M. Calvi, M.J. Kowalsky. *Displacement-based seismic design of structures*. IUSS Press, 2007.

[23] J. McCormick, H. Aburano, M. Ikenaga, M. Nakashima. Permissible residual deformation levels for building structures considering both safety and human elements. *Proceedings of the 14th World Conference on Earthquake Engineering*, Beijing, China, October 12-17, 2008.

[24] Federal Emergency Management Agency. Quantification of building seismic performance factors. *Report FEMA P695*. Federal Emergency Management Agency, 2009.

[25] L.D.A. Wiebe. Design of controlled rocking steel frames to limit higher mode effects. *PhD Dissertation*. University of Toronto, 2013.

[26] M. Pollino, M. Bruneau. Dynamic seismic response of controlled rocking bridge steel-truss piers. *Engineering Structures*, **30**, 1667-1676, 2008.

[27] H.-J. Kim, C. Christopoulos. Friction damped posttensioned self-centering steel moment-resisting frames. *Journal of Structural Engineering*, **134**, 1768-1779, 2008

[28] National Institute of Standards and Technology. Evaluation of the FEMA P-695 methodology for quantification of building seismic performance factors. *Report NIST GCR 10-917-8*. National Institute of Standards and Technology, 2010.

[29] OpenSees. Open system for earthquake engineering simulation (OpenSees), v2.3.2. Pacific Earthquake Engineering Research Center, 2011.